SPECTRA OF THE VELOCITY FLUCTUATIONS IN THE WAKE OF STALLED AIRFOILS

Thesis by

Jay William Stuart, Jr.

In Partial Fulfillment of the Requirements

for the Degree of

Aeronautical Engineer

California Institute of Technology

Pasadena, California

1951

ACKNOWLEDGEMENT

The author of this thesis would like to recognize the invaluable guidance and objective criticisms patiently presented by his advisor, Dr. Hans W. Liepmann. Graditude is also extended to Mr. Phil Lamson (who is carrying on allied investigations) for interested assistance in procuring the testing equipment, putting it in operating order, and for helping to gather and present the data.

Additional recognition is deserved by Mr. Raymond Chuan and Mr. Anatol Roshko, who have much experience in this field, for their constructive suggestions on all phases of this research.

Mr. M. Jessie, the electronics technician, was very patient and direct in his explanation of the operation of the electrical equipment.

Extra thanks are due to the Douglas Aircraft Company, El Segundo Division, for making their repreduction equipment available.

Special appreciation is given here to the author's fiance, Miss Nancy Giovinazzo, for her cheerful and patient assistance in preparing the material.

SYMBOLS

x	Cartesian coordinate in the direction of the free stream flow
y	Cartesian coordinate in the direction normal to the free stream flow and the pitching axis of the airfoil
U_o	free stream velocity -- tunnel velocity
U	total velocity of disturbed flow in direction of U_o
u	fluctuating component in direction of U_o
$\overline{u^2}$	mean square fluctuating velocity or power perturbation in the flow
h	dynamic pressure head of flow in wind tunnel in mm of alcohol
$f(\omega)$	turbulence spectrum power density
c	chord of airfoil
$d = c \sin \alpha$	projection of the chord in U_o direction
$R_c = U_o\, c/\nu$	chord Reynolds number
M	mesh size of the grids
$S = \omega d/U$	Strouhal number
R	resistance of the hot wire at the measuring temperature
R_a	resistance of the hot wire at the room temperature
R_o	resistance of the hot wire at 0^o C
i	heating current in the hot wire
V	voltage across the hot wire
r	reading of the frequency analyser
α	angle of attack of the airfoil relative to U_o direction
ω	frequency of flow fluctuations
ν	kinematic viscosity

ABSTRACT

During the last twenty years a considerable amount of work has been done in order to understand buffeting and the mechanism of the separated flow that causes it. In these investigations the results have either not been clear or they contain some unknown interaction between the indicating apparatus and the flow in the wake. In the present paper one type of the formerly observed flow configurations is investigated by using a properly compensated hot wire anemometer. This technique exhibits some of the results previously obtained but with greater significance and some added phenomena.

INTRODUCTION

On July 21, 1930, the spectacular crash of the Junkers G-AAZK airplane occurred at Meopham, Kent, England. This accident called attention to the phenomenon of buffeting. The buffeting phenomenon was considered to be the resonant vibrations of the tail surfaces of an aircraft with the vortices in the wake from upstream bodies. After an extensive investigation the British concluded that the accident was caused by tail buffeting, and the Germans concluded that it was not. Since then much work has been conducted in England, Germany, and the United States to obtain information about the effects, if any, of separated flow on elastically suspended bodies.

The usual method of most investigators was to establish a separated flow of either the turbulent or vortex street type downstream of a cylinder, flat plate, or simple airfoil. In this flow was placed a flexibly supported lifting body. The forced oscillations of this responding body were recorded. The records were then studied to determine if these oscillations could contribute to buffeting.

A summary of previous results can be found in Goldstein (ref. 1) and in a more recent paper by Krzywoblocki (ref. 2). On the whole the previous experiments resulted in the observation of periodic oscillations in the wake. These vortex patterns have a constant Strouhal number equal to 0.20 in the wake of a cylinder, and 0.15 in the wake of a stalled airfoil at R_c's below the critical values for vortex

streets. The Strouhal number is defined by $S = \frac{\omega d}{U}$, where d is projection of the chord in the free stream direction, ω is the frequency of the regular fluctuation, and U is the mean velocity. There exists an uncertainty about the determination of d for most bodies except for a simple cylinder.

A basic question is now apparent. Does the oscillating body indicator exhibit the true flow fluctuations or does it also include the effects due to the interaction of the indicator with the fluctuating flow Due to its inertia and other dynamic properties, the indicator has a definite lag and will be able to respond significantly only to the fluctuations having similar dynamic properties. These properties of the indicator allow it to respond only to small frequencies and large amplitudes. It follows that it does not indicate general turbulence. Also this type of indicator does not measure local values, since its size and oscillations extend over a relatively large region of the flow. Thus it responds only to large, average effects.

In the present investigation these phenomena were observed in a similar flow by means of an indicator which does not have such limitations. Such an instrument is a properly compensated hot wire anemometer.

PURPOSE

The purpose of these experiments is the determination of the power spectrum of the velocity fluctuations in the wake of a stalled airfoil. This gives a more complete analysis of the fluctuations than has previously been found from the response of an aerodynamic indicator. This power spectrum in fluid flow is described as the distribution of the power per frequency interval, and is analytically defined by

$$\overline{u_\omega^2} = \int_0^\omega f(\omega)\, d\omega \qquad (1)$$

If $\overline{u^2}$ is normalized by the total power in the turbulent fluctuations - $\overline{u^2} = \int_0^\infty f(\omega)\, d\omega$, the resulting ratio - $\frac{\overline{u_\omega^2}}{\overline{u^2}}$ - denotes the fraction of the energy in the turbulent fluctuations in the frequency interval zero to ω. This power spectrum is defined without limitation to either random or the regular fluctuations. The random fluctuations correspond to ordinary turbulence, in which $f(\omega)$ decreases continuously from $f(0)$ at $\omega = 0$, to zero for large ω. For the regular vortex patterns and periodic phenomena $f(\omega_o)$ forms a narrow, pronounced peak at the frequency, ω_o, of the periodic wave or vortex. For an ideal harmonic wave or vortex street

$$f(\omega_o) \longrightarrow \delta(\omega - \omega_o), \qquad (2)$$

where $\delta(\omega - \omega_o)$ is a delta function.

Previous buffet experiments have been concerned mainly with the periodic fluctuations in the wake. The buffeting phenomenon was considered to be a sharp resonance of the empennage structure of an aircraft with the vortex street in the wake. The present experiments were undertaken with the intent of measuring the complete spectrum of the fluctuations in order to ascertain the importance and relative magnitude of both periodic and random fluctuations.

TESTING EQUIPMENT

The testing equipment consisted of a wind tunnel, turbulence grids, two airfoils, a traversing mechanism, hot wire anemometers, and electrical measuring apparatus.

WIND TUNNEL

The wind tunnel is an open circuit type, powered by a direct-current motor. The flow through the 20 in. x 20 in. x 20 ft., parallel channel has a variable operating speed with a higher limit of 50 f.p.s. and a low turbulence level of approximately .03 percent in the working region. The speed of the flow in the tunnel is measured by a micromanometer, which indicates the dynamic pressure head - h - in millimeters of alcohol. The channel has a removable upper wall so that the test section was readily accessible.

At the upstream end of the working region two transverse slots, which are 20 inches apart, were designed into the tunnel to expedite the changing of models and to provide for convenient control of the free stream turbulence by a set of standard grids. See diagram of test set-up (fig. 1).

TURBULENCE GRIDS

To obtain a certain turbulence level, one of these grids is inserted into a slot which is located upstream of the airfoil and hot wire. Each grid consists of a wire mesh installed in a square wooden frame. The inner edges of the frames are flush with the walls of the tunnel. From the set available, 3 grids, designated as fine, no. 6, and no. 4, were used. The fine, no. 6, and no. 4 grids have

meshes, M, of .05, .17, and .25 inches each and an open area of approximately ninety percent.

MODELS

The two, 2-dimensional models have chords of 3.5 inches and 7.00 inches. The 3.5 inch chord airfoil is shaped by rounding off the leading edge and symmetrically beveling to a sharp trailing edge the aft 33 percent of an 11.2 percent thick flat board. The 7.00 inch chord model is a simple symmetrical airfoil of 11.8 percent thickness.

Each airfoil is supported horizontally in a frame which is similar to a grid frame. The frame and model are conveniently inserted into the flow through one of the covered slots. Each model also has an adjustable angle of attack in approximately 15° increments.

TRAVERSING MECHANISM

The traversing mechanism was improvised from a lead screw type micromanometer, whose accuracy of 1/10 mm, is far greater than this work requires. It was placed on the top of the tunnel. The length of the lead screw readily allowed a vertical traversing range of 15 inches. A single sting type mount with a semi-cylindrical saddle was attached to the lower end of the traversing extension. The cylindrical glass hot wire holder was held snugly in this saddle with elastic bands cut from rubber tubing. Besides being convenient, this manner of securing the holder also helped in damping out possible external vibrations, which never were observed.

HOT WIRES

The hot wire anemometer, the indicating apparatus, generally is constructed in two manners in this laboratory. The holders are either cylindrical ceramic rods with two or four symmetrically located longitudinal holes, through which non-insulated copper wire leads are inserted, or glass tubing, which contains two or four insulated copper wire leads. One end of each wire is formed like the prong of a fork. To it is soldered a needle probe, on whose point is attached a hot wire.

The hot wires are either tungsten or platinum. They require processing before soldering on the probe. The tungsten wire, the stronger of the two, must be copper plated before it can be soldered. Also it is conveniently welded if the equipment is available. The platinum wire is delivered with a protective silver coating which is etched off with nitric acid. The temperature coefficients of resistivity of the two materials are .0035 for platinum and 0.0045 for tungsten. All of the present data were collected with a .0002 inch diameter by 0.16 inch long, platinum wire installed in a glass holder. Much preliminary work was done with the other varieties of hot wires. The data on the hot wire are shown in figure(2). Additional information about hot wires may be found in reference (3).

ELECTRICAL APPARATUS

The electrical apparatus consists of three,6 volts lead storage batteries, a Wheatstone bridge, a potentiometer, a compensated amplifier, a square wave generator, an oscillator, an oscilloscope,

an a.c. power supply, a r.m.s. voltmeter, and a Hewlett-Packard frequency analyser.

The current from two of the batteries is used to heat the hot wire. The Wheatstone bridge is used to regulate the heating current and thus the temperature of the hot wire. The potentiometer is used to measure this current and the mean voltage. This is the only equipment required to calibrate and use the hot wire for mean flow measurement.

The amplifier has a maximum gain of 1400. The gain can be changed by a factor of 2 for each of 9 selector positions. The amplifier has one 6 volt battery and an alternating current power supply system. The amplifier also includes a stage to compensate for the thermal lag of the hot wire response. It has an accuracy of 3 percent for frequencies between 10 and 10,000 cycles per second. The oscilloscope is used in conjunction with the square wave generator to observe the response to the flow fluctuations qualitatively and to adjust the compensation. This response can be switched to the frequency analyser, where the magnitude of the voltage response is measured with a moderately damped r.m.s. voltmeter. This equipment is used to measure the turbulence spectrum at all significant frequencies greater than 20 cps. The instrument has decreasing accuracy below 20 cps.

RESULTS

The measurement of a complete power spectrum of the fluctuating velocities in the wake of a stalled airfoil by means of a hot wire anemometer was successful from the beginning; spectra are presented for all pertinent configurations. The majority of these configurations consisted of the hot wire traverses across the wake for R_c = 0.5 and 1.5 x 10^5 and α = 32 and -22 degrees respectively. Some further investigations were made at different free stream turbulence levels. In every case the power spectrum contained sharp peaks superimposed upon a normal turbulence spectrum. The periodic fluctuations corresponding to the peaks were generally of the same order of magnitude as the turbulent fluctuations.

These spectra are presented graphically as $f(\omega)/\overline{u^2}$ versus ω in the appendix. The scatter of the data is not appreciable. The positions of the peaks are accurate to about 5 cps. Their amplitudes appear to be accurate to 5 percent.

The regular fluctuations having the lowest frequency are similar to the vortex streets found in previous work. They appear in a pattern which is symmetrical about the middle of the wake, as illustrated in the plots of the amplitudes at these predominant frequencies through the wake (fig. 5 and 6) for the two Reynolds numbers. At both R_c's the Strouhal number is 0.28 for these low frequency oscillations. This value of S is higher than in most previous measurements. This is probably because these tests were conducted in a higher R_c range and the widths of the wakes which correspond to the vortex street

depend on the particular shape and angle of attack of the airfoil.

Additional regular fluctuations existing at different frequencies were also found. There are insufficient data to identify some of them. But for each of the two sets of runs mentioned above there was a definite higher frequency fluctuation. This fluctuation exists in the center of the wake and gives a constant S = 0.44. It is possible that this wave is due to the effects of the two sets of vortices at the lower frequency. If this is true, the reason that the S for the high frequency fluctuation is less than twice the S for the low frequency is not known.

For $R_c = 1.5 \times 10^5$ a third predominant wave appears consistently at an intermediate frequency for most of the traversing stations. But due to their smaller magnitude and to the lack of data no definite conclusions can be stated about them. Some of the spectra which have these peaks are in figures (19) to (24).

A verification of the existence of these regular fluctuations superimposed on turbulence and of their dependence on being in the wake of a stalled airfoil was found by observing that there were no regular fluctuations in the flow, after translating the hot wire into a region outside of the wake or after decreasing the angle of attack to zero.

Since the operating Reynolds numbers were small, grids were inserted into the upstream flow to give a higher effective R_c and earlier transition in the boundary layer, which causes the position

of the separation to change. This increase in turbulence had a negligible effect. Moreover, the vortices exhibited no perceptible change in the amount of their diffusion due to the varied turbulence level at three chord lengths downstream of the airfoil. The effects of the change in turbulence are shown in figure (4). Also plots of the turbulence power spectrum for the grids alone were taken from reference (4) and are presented in figure (3).

The total pressure heads through the wakes were measured to show the mean velocity distribution. These total head profiles are drawn to a small scale and are presented on each of the related turbulence spectrum graphs. These small graphs, together with sketches of the model and hot wire, give a picture of their relative positions.

CONCLUSION

Measurements of the power spectrum of the velocity fluctuations have been made. It is shown that the complete spectrum consists of the spectrum corresponding to a regular vortex street and other unfamiliar regular fluctuations superimposed upon a normal turbulence spectrum. An increase in the free stream turbulence level was found to have a negligible effect on the observed wake pattern.

Further investigations at higher R_c's and in a larger tunnel are recommended in order to determine whether the pattern of regular fluctuations disappears completely at higher R_c's. A more detailed investigation far downstream of the airfoil may be useful.

Furthermore, an investigation of the response of an elastically supported lifting surface in wake flow of known characteristics should be investigated.

REFERENCES

1. Goldstein, S., "Modern Developments in Fluid Dynamics." Clarendon Press, Oxford, England (1938), Vols. I and II, pp. 37, 421.

2. Krsywoblocki, M.Z., "Investigation of the Wing Wake Frequency with Application of the Strouhal Number." Journal of the Aeronautical Sciences, Jan. 1945, pp. 51-62.

3. Willis, J.B., "Review of Hot Wire Anemometry." ACA-19, Oct. 1945 (Australian).

4. Liepmann, H.W., Laufer, J., and Liepmann, K., "Spectrum of Isotropic Turbulence." GALCIT Report, July 1949.

5. Frazer, R.A., and Duncan, W.K., "Two Reports on Tail Buffeting." Reports and Memoranda 1457 (1932) Vol. I, pp. 528-562, (British).

APPENDIX

REDUCTION OF DATA

The reduction of the electrical data to flow data needs some illumination. The mean flow velocity was found from a modified form of King's equation, when the current was varied and the resistance was held constant. The modified King's equation becomes

$$\frac{i^2 \alpha R R_o}{R - R_a} = a + b\sqrt{U} \tag{3}$$

The constants may be evaluated by measuring the slope and intercept of a plot of i^2 against $\sqrt{U}$. See figure (2) and reference (3).

The spectra data are the readings from a frequency analyser. These readings correspond to the root mean square of the fluctuations existing in a finite band of frequencies. In taking the r.m.s. value the analyser integrates a power density response, $f(\omega)$, over the finite band of frequencies. This r.m.s. reading, r, may be conceived as being the product of an unknown electrical sensitivity, s, and an unknown area factor, A, which is characteristic of the manner in which the analyser determines the mean value. In symbolic form the reading may be expressed as follows:

$$r_\omega^2 = s \int_{\omega-\epsilon}^{\omega+\epsilon} f(\omega)\, d\omega, \tag{4}$$

which gives $r_\omega^2 = sA\,\overline{f(\omega)}$. The integration of $f(\omega)$ with respect to from zero to infinity corresponds to the total mean turbulent power at a point in the wake. This quantity is expressed as

$$\int_0^\infty sA\, f(\omega)\, d\omega = \int_0^\infty r_\omega^2\, d\omega = sA\,\overline{u^2} \tag{5}$$

Now normalizing with the total power, the proportion of the turbulent power density at any frequency in the spectrum may be formulized as follows:

$$\frac{f(\omega)}{\overline{u^2}} \qquad \frac{r_\omega^2}{\int_0^\infty r_\omega^2 \, d\omega} \tag{6}$$

Thus the proportion of the power density in the spectra may be found by squaring the readings, reduced to one sensitivity and dividing by the integral of the squared readings over all frequencies. This is the form in which the results are presented.

FIGURE 1

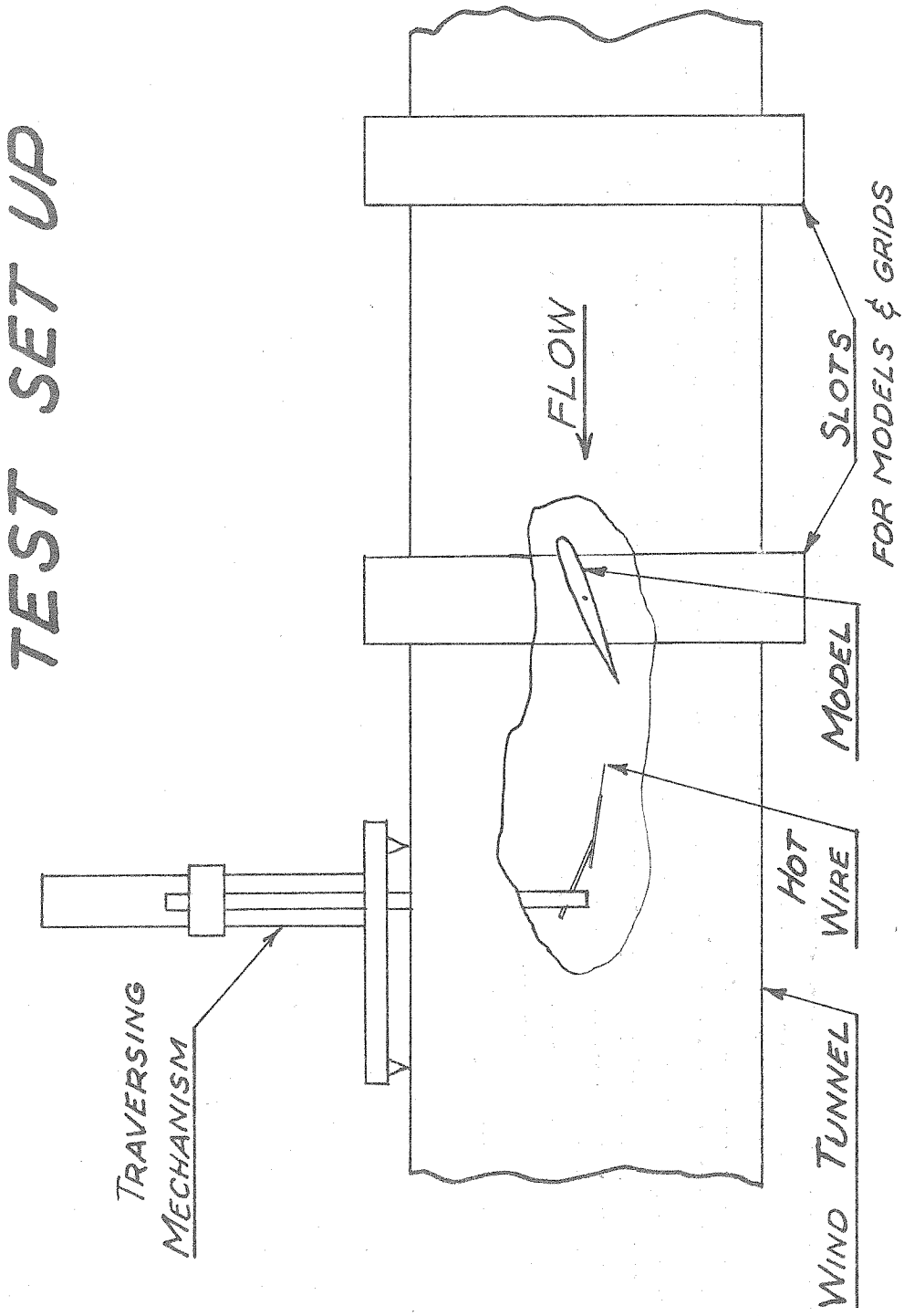
TEST SET UP
FLOW
SLOTS FOR MODELS & GRIDS
MODEL
HOT WIRE
WIND TUNNEL
TRAVERSING MECHANISM

FIGURE 2

HOT WIRE CALIBRATION CURVE

DESCRIPTION OF HOT WIRE:

MATERIAL PLATINUM — R_i = 18.78 OHMS

DIAMETER 0.0002 INCH — R_a = 20.10 OHMS

LENGTH 0.160 INCH — R = 38.60 OHMS

OPERATING TEMPERATURE — 290 °C

CALIBRATION CONSTANTS: $\frac{R-R_a}{l^2\alpha RR_a} a = 1.232 \times 10^{-3}$ & $\frac{R-R_a}{l^2\alpha RR_a} b = 3.45 \times 10^{-4}$

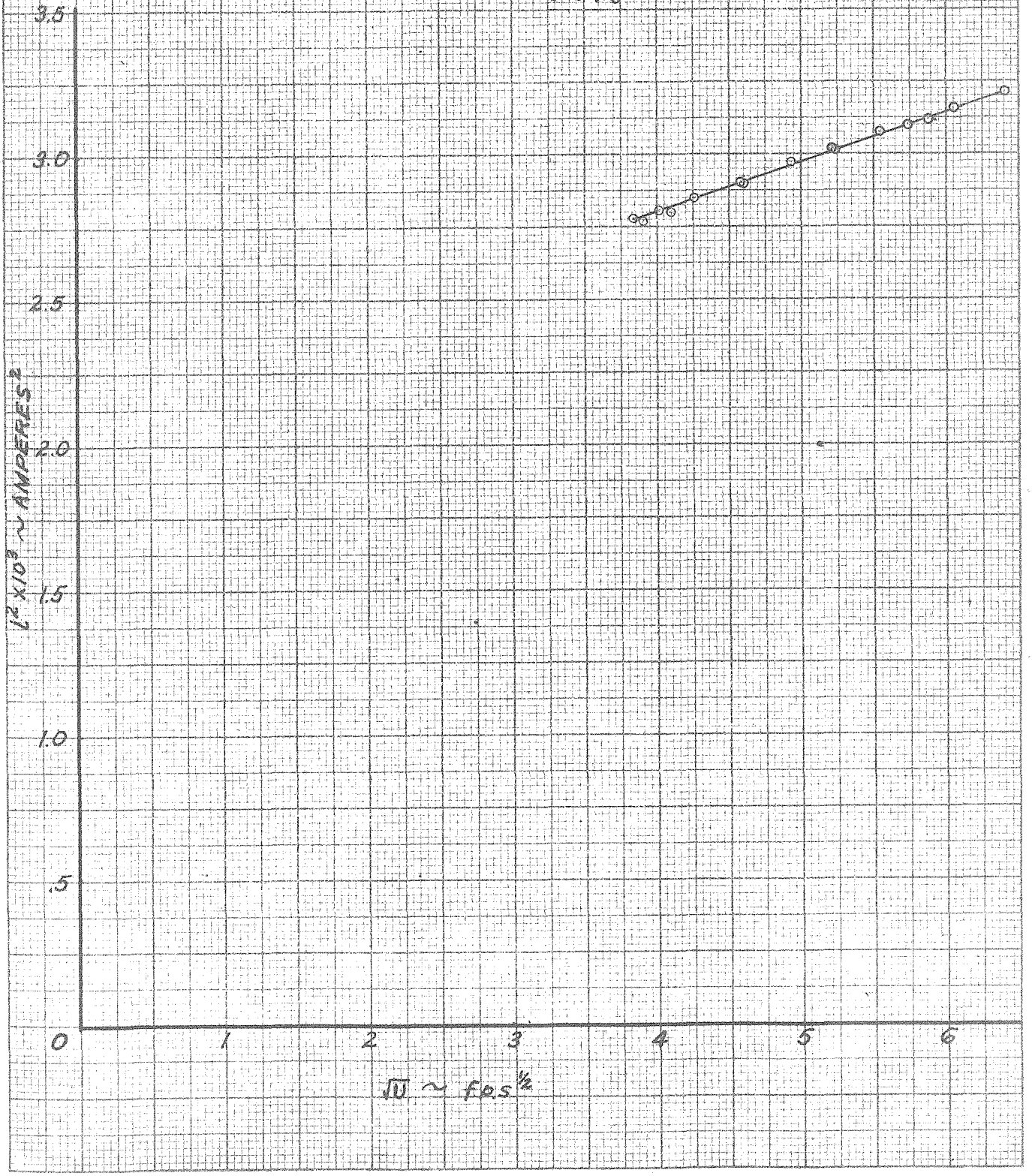

FIGURE 3

NORMALISED TURBULENCE SPECTRA OF GRIDS

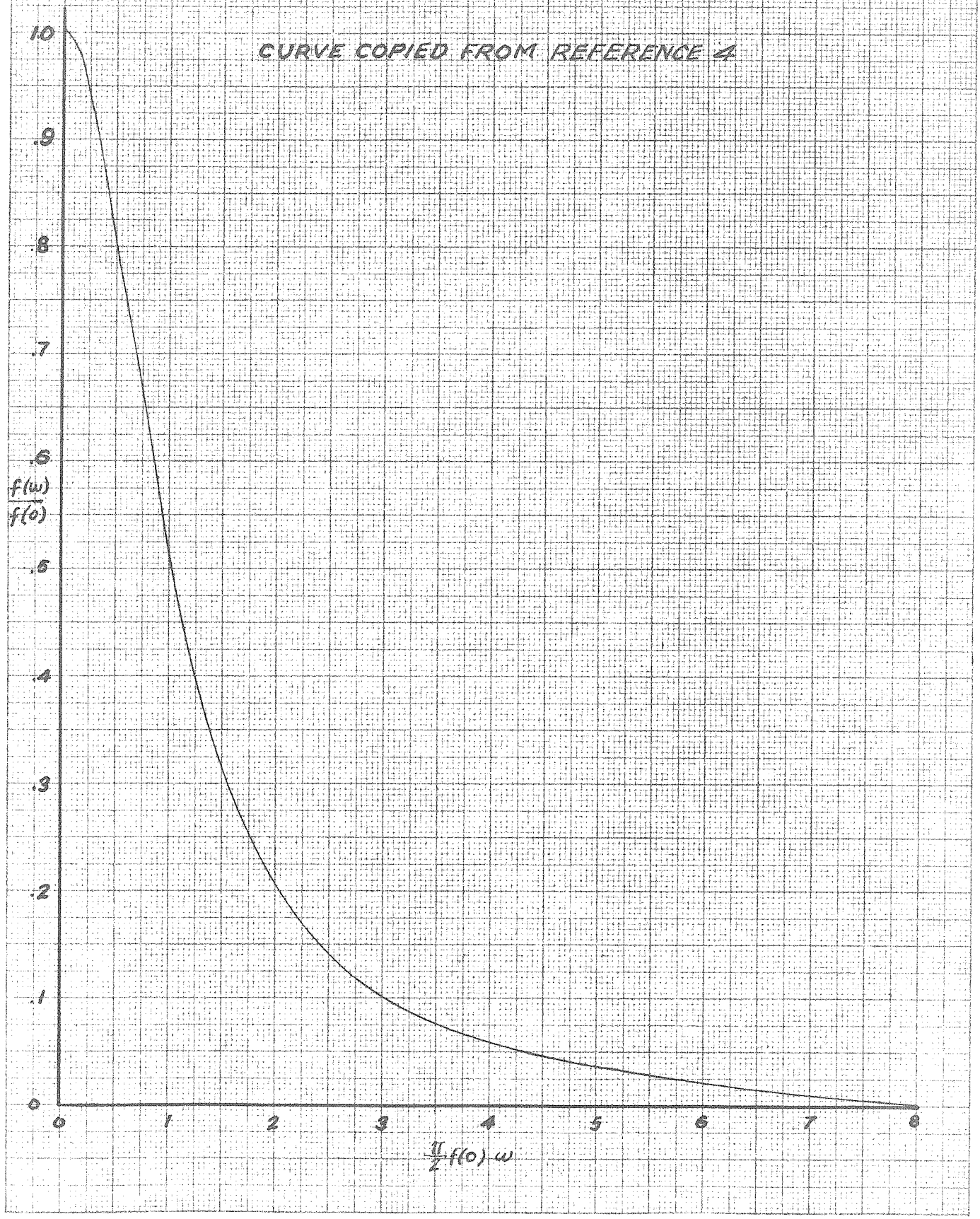

FIGURE 4

TURBULENCE SPECTRUM IN WAKE

GRID COMPARISON

$h = 13.65$ mm

$X = 2\frac{5}{8}\,C$, $Y = 0.00$

$C = 7.00$, $\alpha = 21.5°$

$R_C = 1.63 \times 10^5$

SYMBOL	GRID
⊙	NO. 6
⊡	NONE

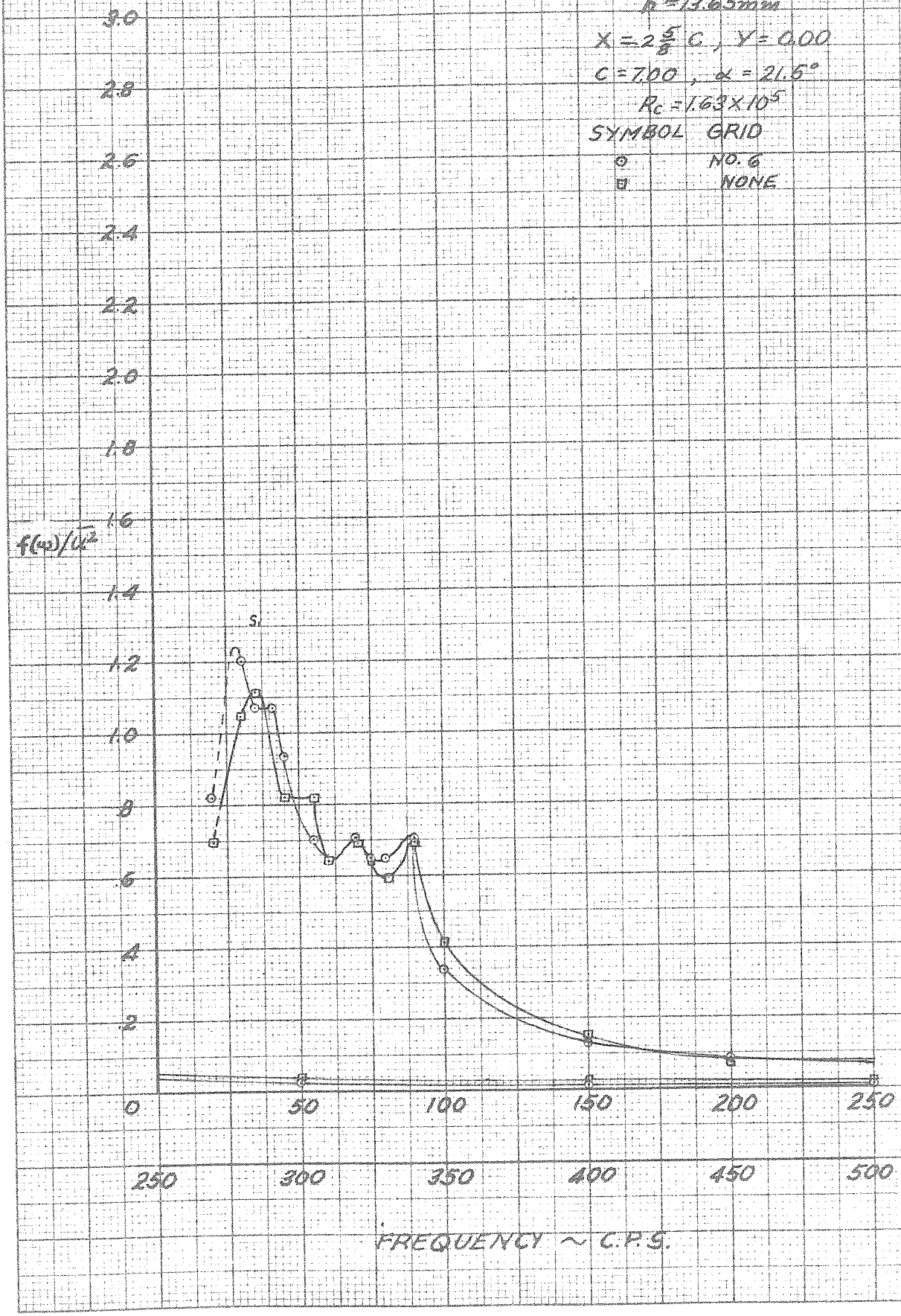

FIGURE 5

AMPLITUDES THRU WAKE OF PREDOMINANT FREQUENCIES

$C = 3.50$ in. , $h = 4.87$ mm, $\alpha = 32.0°$

$R_c = 1.49 \times 10^5$, $X = 3\,C$, FINE GRID

$S_1 = .28$, $S_2 = .44$

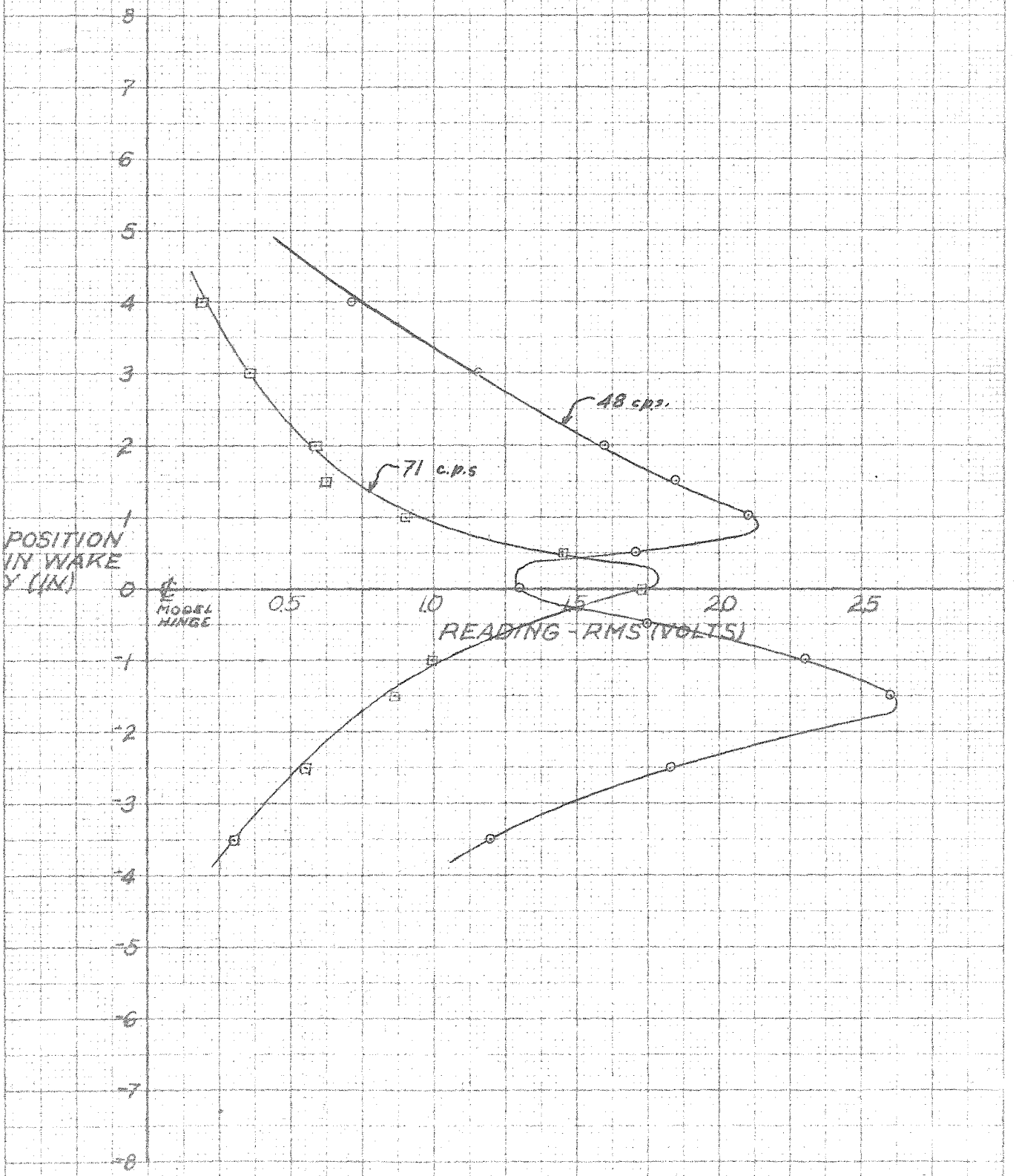

FIGURE 6

AMPLITUDES THRU WAKE OF PREDOMINANT FREQUENCIES

$C = 7.00$ in , $h = 11.10$ mm, $\alpha = -22.0°$

$R_c = 1.47 \times 10^5$, $X = 2\frac{5}{8}\,C$, NO GRID

$S_1 = .28$ $S_2 = .44$

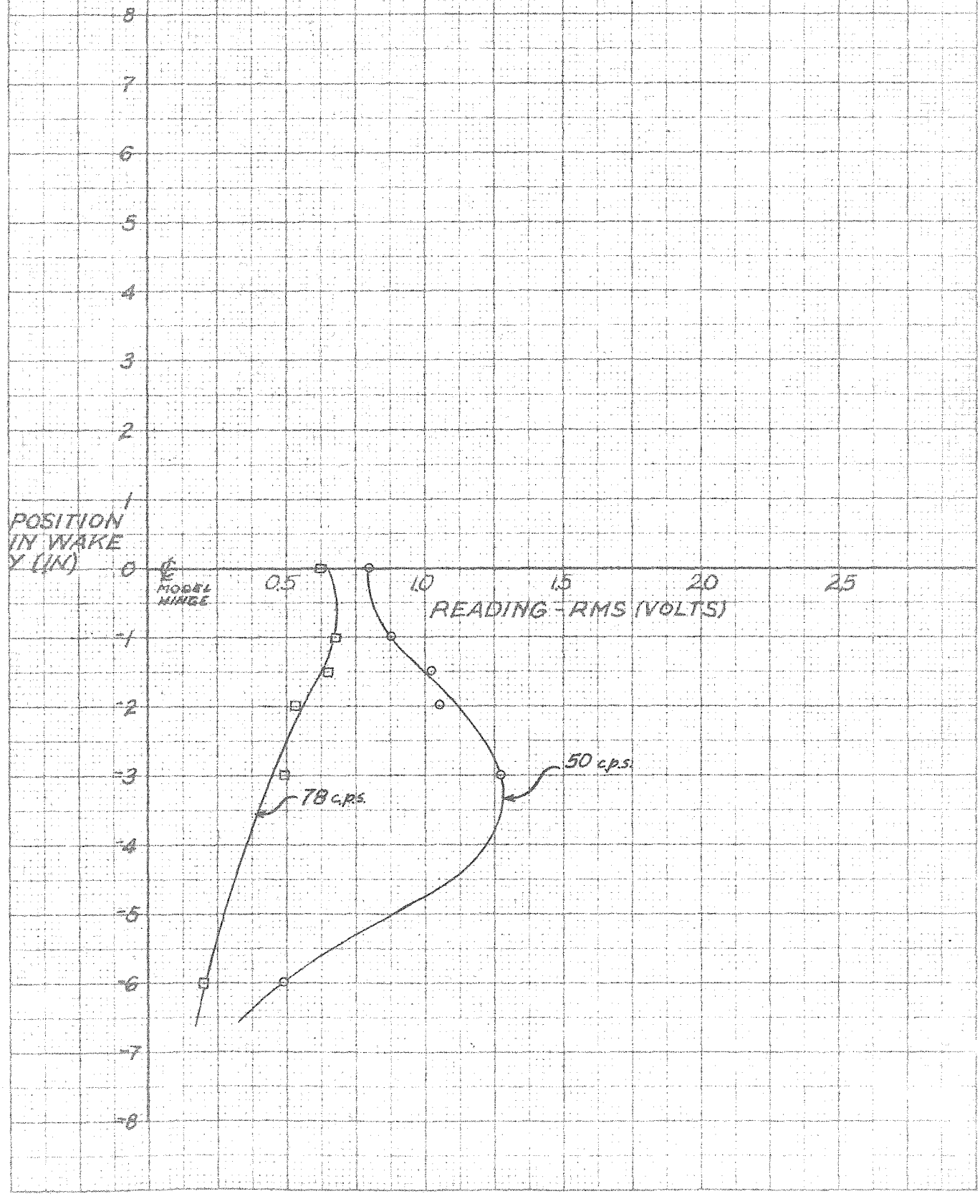

FIGURE 7

TURBULENCE SPECTRUM IN WAKE

C = 3.50 in., h = 4.87 mm, α = 32.0°

X = 36, Y = 0.00 in., FINE GRID

S_1 = 30, S_2 = 40

R_c = .49 X 10^5

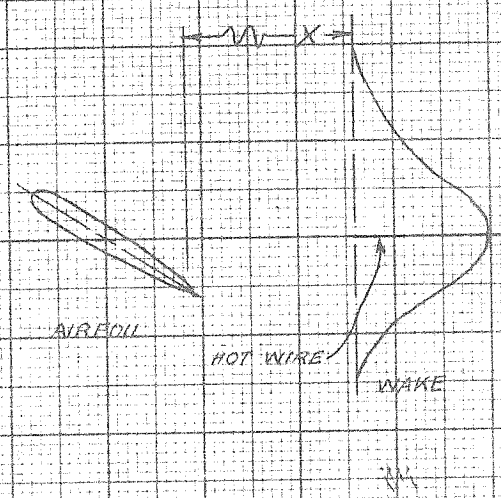

$f(w)/\overline{u^2}$

3.0
2.8
2.6
2.4
2.2
2.0
1.8
1.6
1.4
1.2
1.0
.8
.6
.4
.2
0

50 100 150 200 250

250 300 350 400 450 500

FREQUENCY ~ C.P.S.

FIGURE 8

TURBULENCE SPECTRUM IN WAKE

C = 3.50 in., h = 4.87 mm., α = 32.0°

X = 3C , Y = 0.50 in., FINE GRID

S_1 = .28 , S_2 = .42

$R_c = 4.9 \times 10^5$

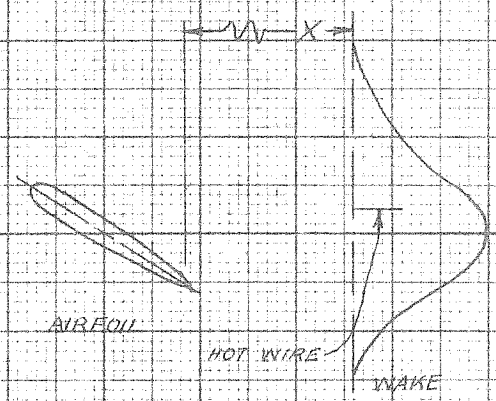

$f(\omega)/\bar{U}^2$

S_1

S_2

3.0
2.8
2.6
2.4
2.2
2.0
1.8
1.6
1.4
1.2
1.0
.8
.6
.4
.2
0

50 100 150 200 250

250 300 350 400 450 500

FREQUENCY ~ C.P.S

FIGURE 9

TURBULENCE SPECTRUM IN WAKE

C = 3.50 in., h = 4.87 mm, α = 32.0°

X = 36 , Y = 1.00 in., FINE GRID

S_1 = .28 , S_2 = .42

R_c = .49 X 10^5

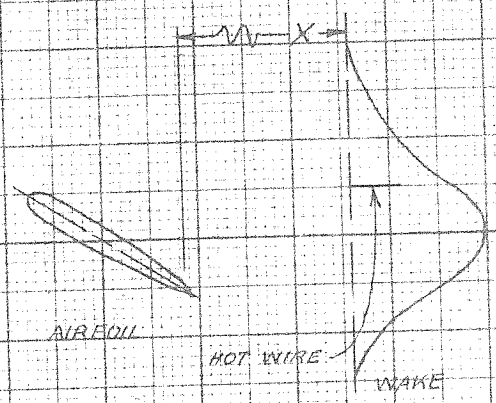

$f(w)/\overline{U^2}$

4.0
3.0
2.8
2.6
2.4
2.2
2.0
1.8
1.6
1.4
1.2
1.0
.8
.6
.4
.2
0

S_1
S_2

0 50 100 150 200 250

250 300 350 400 450 500

FREQUENCY ~ C.P.S

FIGURE 10

TURBULENCE SPECTRUM IN WAKE

C = 3.50 in, h = 4.87 mm, α = 32.0°
X = 3C , Y = 1.50 in , FINE GRID
S_1 = .29 , S_2 = .50
R_c = .49 X 10^5

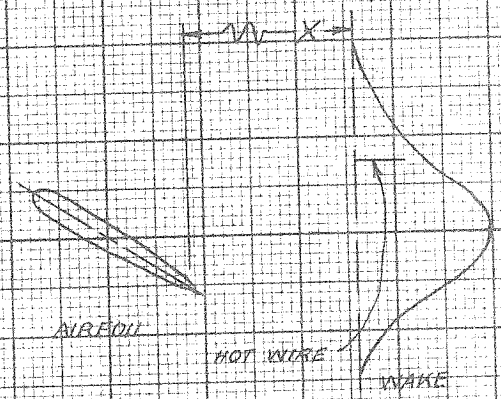

$f(\omega)/\overline{U}^2$

4.0
3.0
2.8
2.6
2.4
2.2
2.0
1.8
1.6
1.4
1.2
1.0
.8
.6
.4
.2
0

S_1
S_2

0 50 100 150 200 250
250 300 350 400 450 500

FREQUENCY ~ C.P.S

FIGURE 11

TURBULENCE SPECTRUM IN WAKE

C = 3.50 in., h = 4.87 mm., α = 32.0°
X = 3C , Y = 2.00 in., FINE GRID
S_1 = .30 , S_2 = .40
R_c = .49 X 10^5

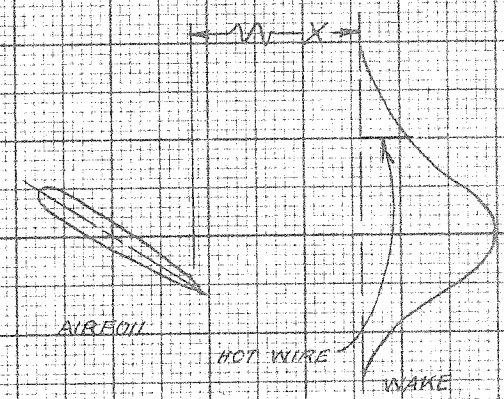

$f(\omega)/\overline{U}^2$

4.0
3.0
2.8
2.6
2.4
2.2
2.0
1.8
1.6
1.4
1.2
1.0
.8
.6
.4
.2
0

S_1
S_2

0 50 100 150 200 250

250 300 350 400 450 500

FREQUENCY ~ C.P.S.

FIGURE 12

TURBULENCE SPECTRUM IN WAKE

C = 3.50 in., h = 4.87 mm, α = 32.0°
X = 36, Y = 3.00 in., FINE GRID
S_1 = .31, S_2 = —
R_c = .49 X 10^5

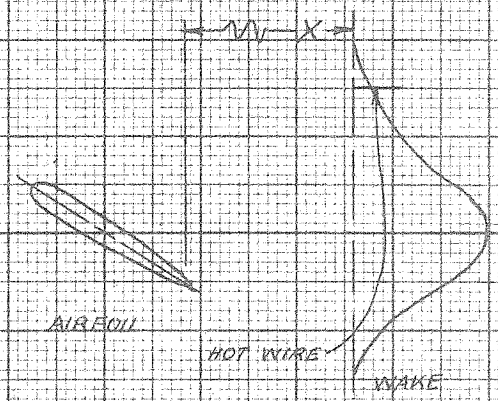

$\overline{F(w)}/\overline{U}^2$

4.0
3.0
2.8
2.6
2.4
2.2
2.0
1.8
1.6
1.4
1.2
1.0
.8
.6
.4
.2
0

50 100 150 200 250

250 300 350 400 450 500

FREQUENCY ~ C.P.S

FIGURE 13

TURBULENCE SPECTRUM IN WAKE

C = 3.50 in, h = 4.87 mm, α = 32.0°

X = 3C, Y = 4.00 in, FINE GRID

S_1 = .31, S_2 = .47

R_c = 4.9 X 10^5

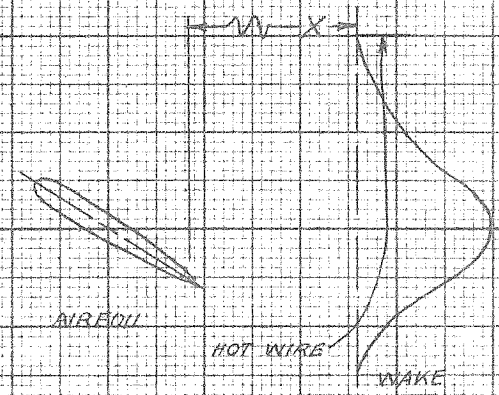

$\overline{u^2}/U^2$

4.0
3.0
2.8
2.6
2.4
2.2
2.0
1.8
1.6
1.4
1.2
1.0
.8
.6
.4
.2
0

S_1
S_2

0 50 100 150 200 250

250 300 350 400 450 500

FREQUENCY ~ C.P.S

FIGURE 14

TURBULENCE SPECTRUM IN WAKE

C = 3.50 in., h = 4.87 mm, α = 32.0°
X = 36 , Y = -0.50 in., FINE GRID
S_1 = ——— , S_2 = .46
R_c = 49 X 10^5

FIGURE 15

TURBULENCE SPECTRUM IN WAKE

C = 3.50 in, h = 4.87 mm, α = 32.0°
X = 3C , Y = -1.00 in , FINE GRID
S_1 = .28 , S_2 = .43
R_c = .49 X 10^5

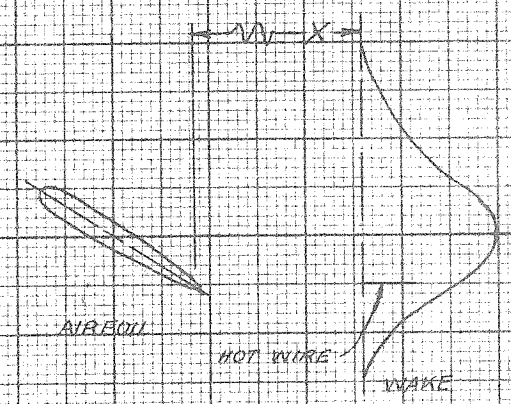

$f(w)/\overline{U}^2$

4.0
3.0
2.8
2.6
2.4
2.2
2.0
1.8
1.6
1.4
1.2
1.0
.8
.6
.4
.2
0

S_1
S_2

0 50 100 150 200 250

250 300 350 400 450 500

FREQUENCY ~ C.P.S

FIGURE 16

TURBULENCE SPECTRUM IN WAKE

C = 3.50 in, h = 4.87 mm, α = 32.0°
X = 36 , Y = -1.50 in , FINE GRID
S_1 = .28 , S_2 = .47
R_c = 4.9 X 10^5

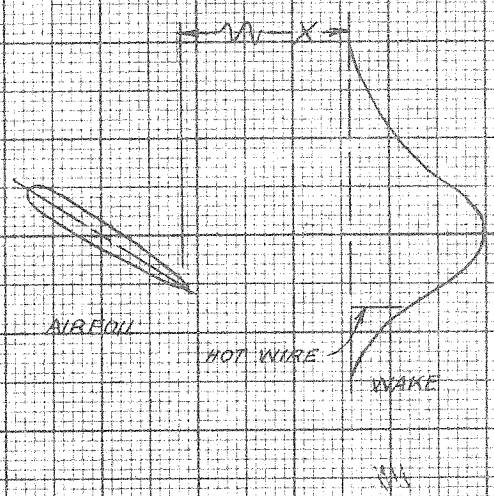

$f(w)/\bar{U}^2$

4.0
3.8
2.8
2.6
2.4
2.2
2.0
1.8
1.6
1.4
1.2
1.0
.8
.6
.4
.2
0

S_1

50 100 150 200 250

250 300 350 400 450 500

FREQUENCY ~ C.P.S

FIGURE 17

TURBULENCE SPECTRUM IN WAKE

C = 3.50 in, h = 4.87 mm, α = 32.0°
X = 3C, Y = 2.50 in, FINE GRID
S_1 = .31, S_2 = .47
R_c = .49 X 10^5

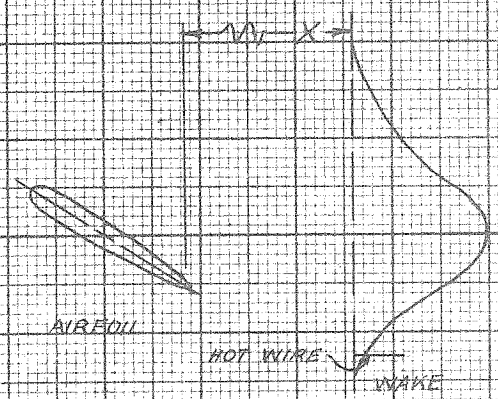

$\overline{f(\omega)} \angle \overline{U^2}$

4.0
3.0
2.8
2.6
2.4
2.2
2.0
1.8
1.6
1.4
1.2
1.0
.8
.6
.4
.2
0

S_2

0 50 100 150 200 250
250 300 350 400 450 500

FREQUENCY ~ C.P.S

FIGURE 18

TURBULENCE SPECTRUM IN WAKE

C = 3.50 , h = 4.87 mm , α = 32.0°

X = 36 , Y = -3.50 in., FINE GRID

S_1 = .29 , S_2 = —

R_c = .49 X 10^5

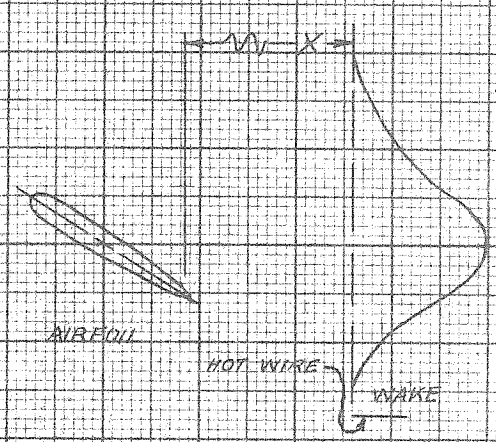

$f(\omega)/\overline{U}^2$

4.0
3.0
2.8
2.6
2.4
2.2
2.0
1.8
1.6
1.4
1.2
1.0
.8
.6
.4
.2
0

50 100 150 200 250

250 300 350 400 450 500

FREQUENCY ~ C.P.S

FIGURE 19

TURBULENCE SPECTRUM IN WAKE

C = 7.00 in, h = 11.10 mm, $\alpha = -22.0°$

X = 2 5/8 C, Y = 0.00 in, NO GRID

$S_1 = .32$, $S_2 = .41$

$R_c = 1.47 \times 10^5$

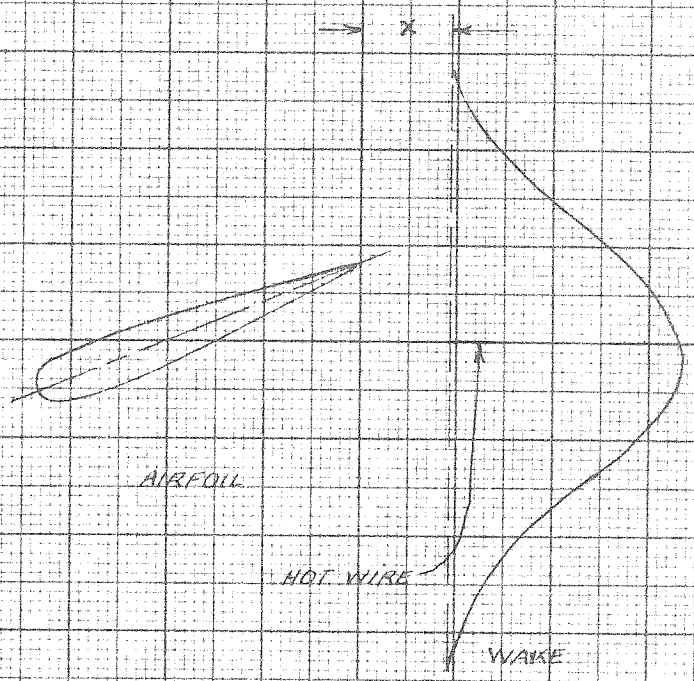

$f(w) / \overline{u^2}$

3.0
2.8
2.6
2.4
2.2
2.0
1.8
1.6
1.4
1.2
1.0
8
6
4
2
0

S_1 S_2

50 100 150 200 250

250 300 350 400 450 500

FREQUENCY ~ C.P.S.

FIGURE 20

TURBULENCE SPECTRUM IN WAKE

C = 7.00 in., h = 11.10 mm, $\alpha = -22.0°$

X = 2 5/8 C, Y = -1.00 in., NO GRID

$S_1 = .28$, $S_2 = .45$

$R_c = 1.47 \times 10^5$

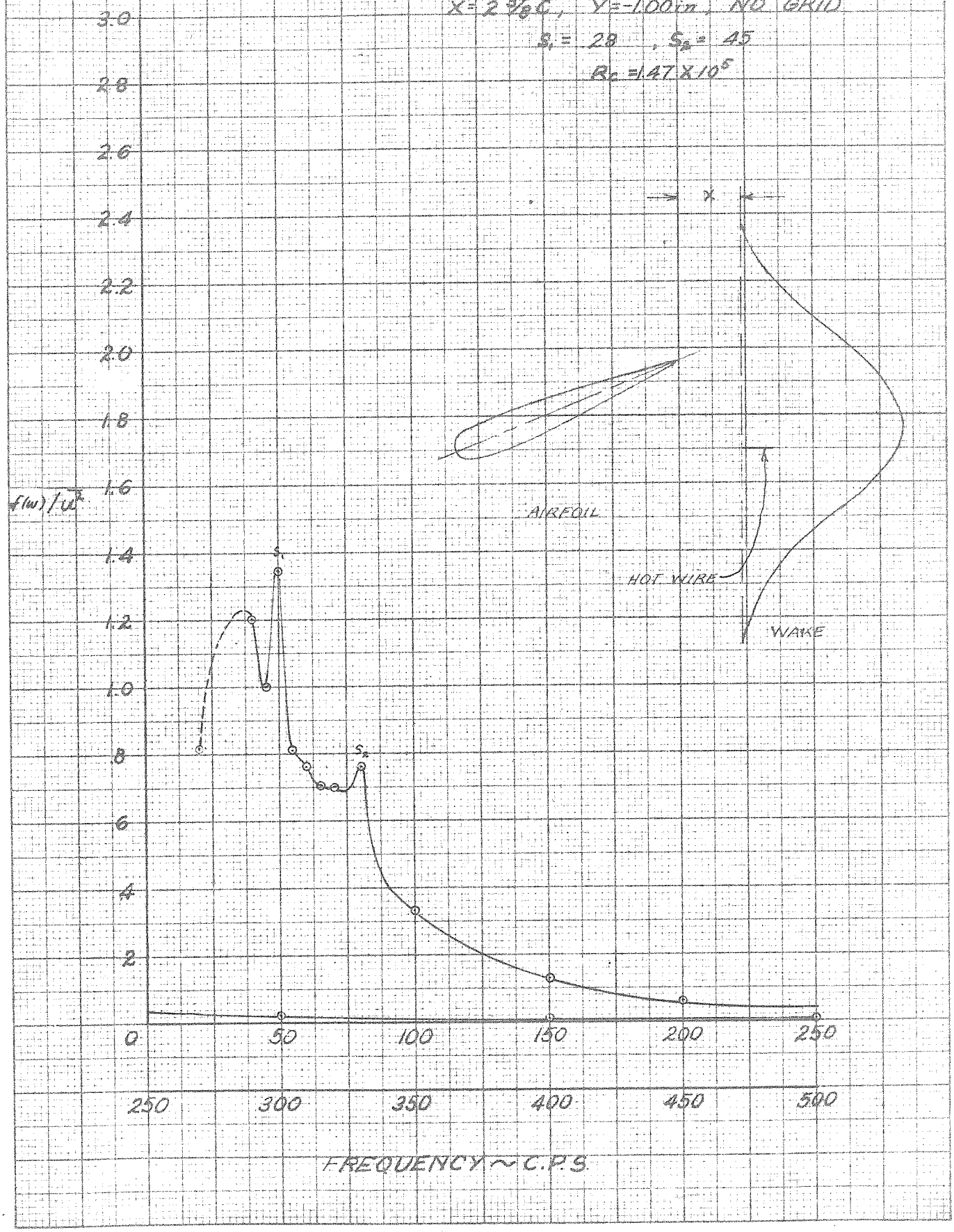

FIGURE 21

TURBULENCE SPECTRUM IN WAKE

C = 7.00 in, h = 11.10 mm, α = -22.0°

X = 2 5/8 C, Y = -1.50 in, NO GRID

S_1 = .27, S_2 = .44

R_c = 1.47 X 10^5

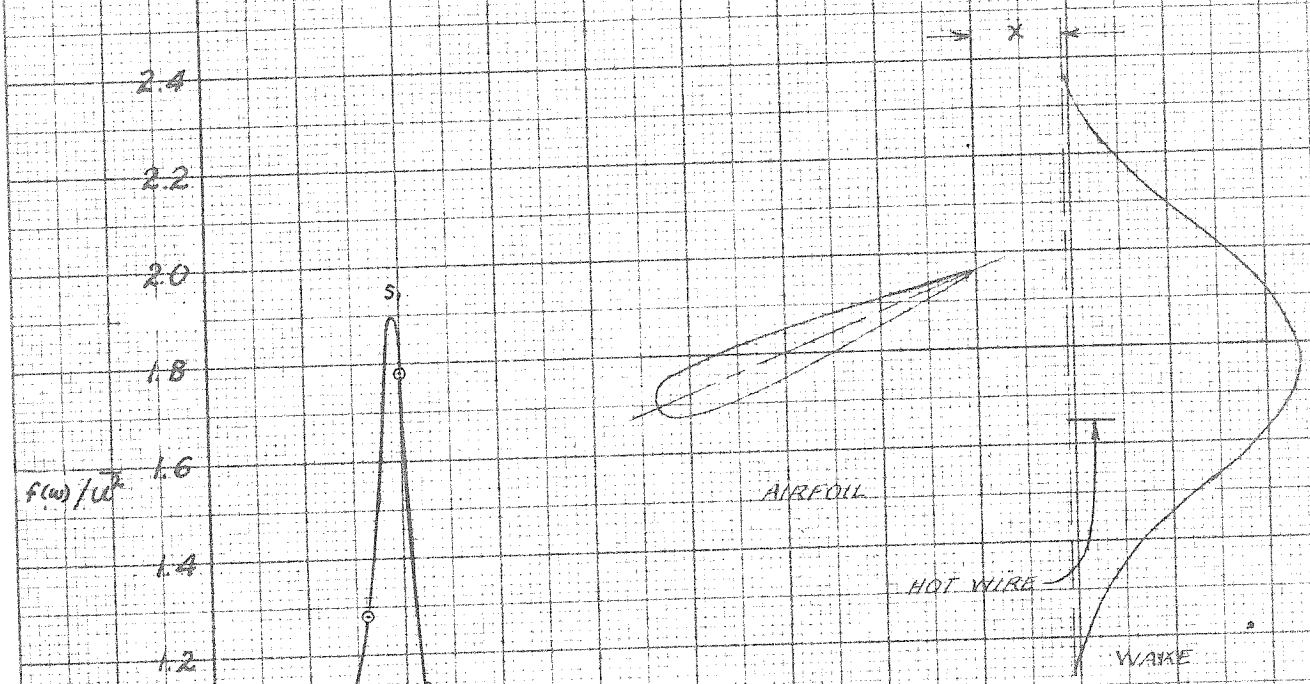

FIGURE 22

TURBULENCE SPECTRUM IN WAKE

C = 7.00 in. h = 11.10 mm, $\alpha = -22.0°$

X = 2 5/8 C, Y = -2.00 in. NO GRID

$S_1 = .28$, $S_2 = ---$

$R_c = 1.47 \times 10^5$

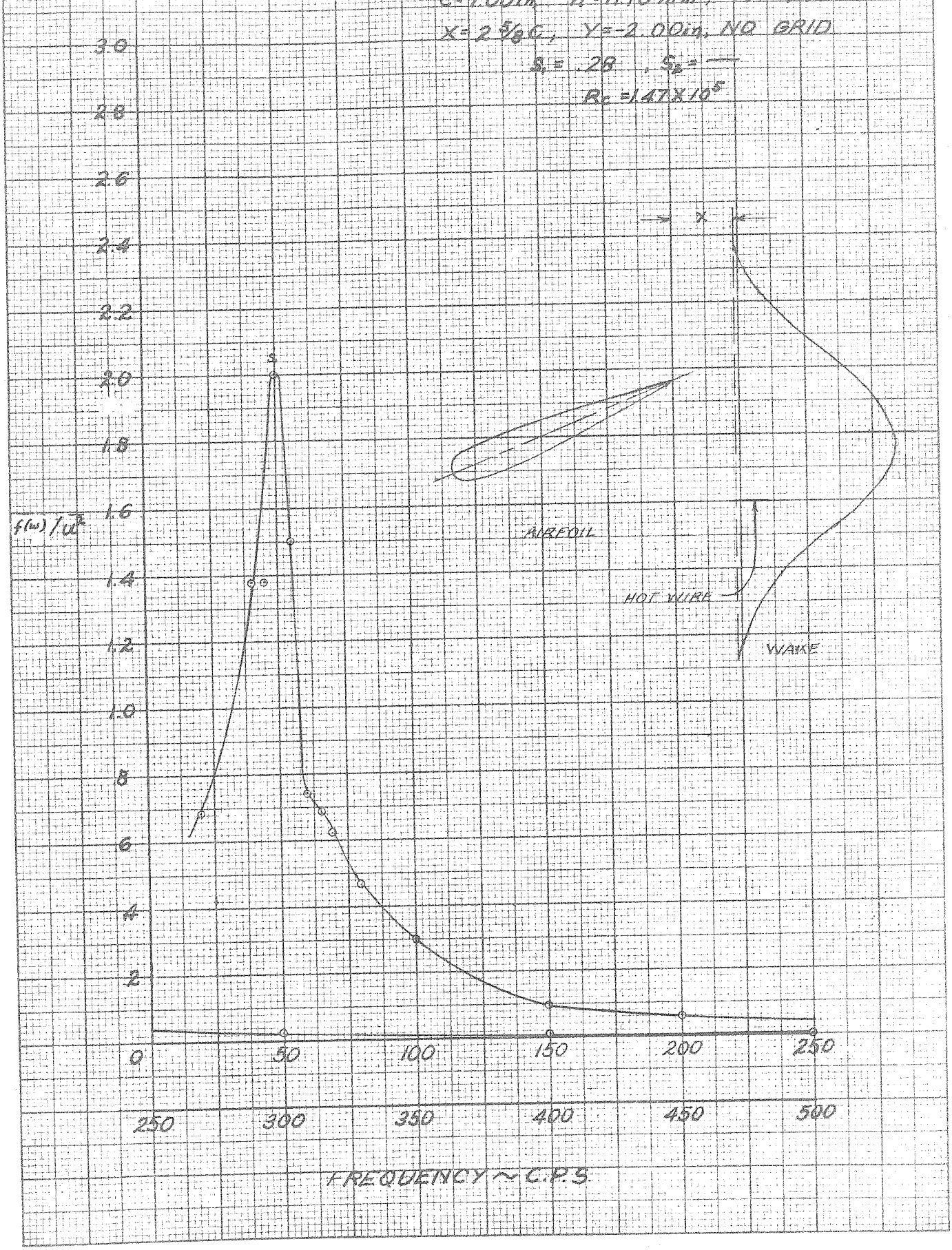

FIGURE 23

TURBULENCE SPECTRUM IN WAKE

C = 7.00 in., h = 11.10 mm., α = -22.0°

X = 2 5/8 C, Y = -3.00 in. NO GRID

S_1 = 27 , S_2 = 44

R_c = 1.47 X 10^5

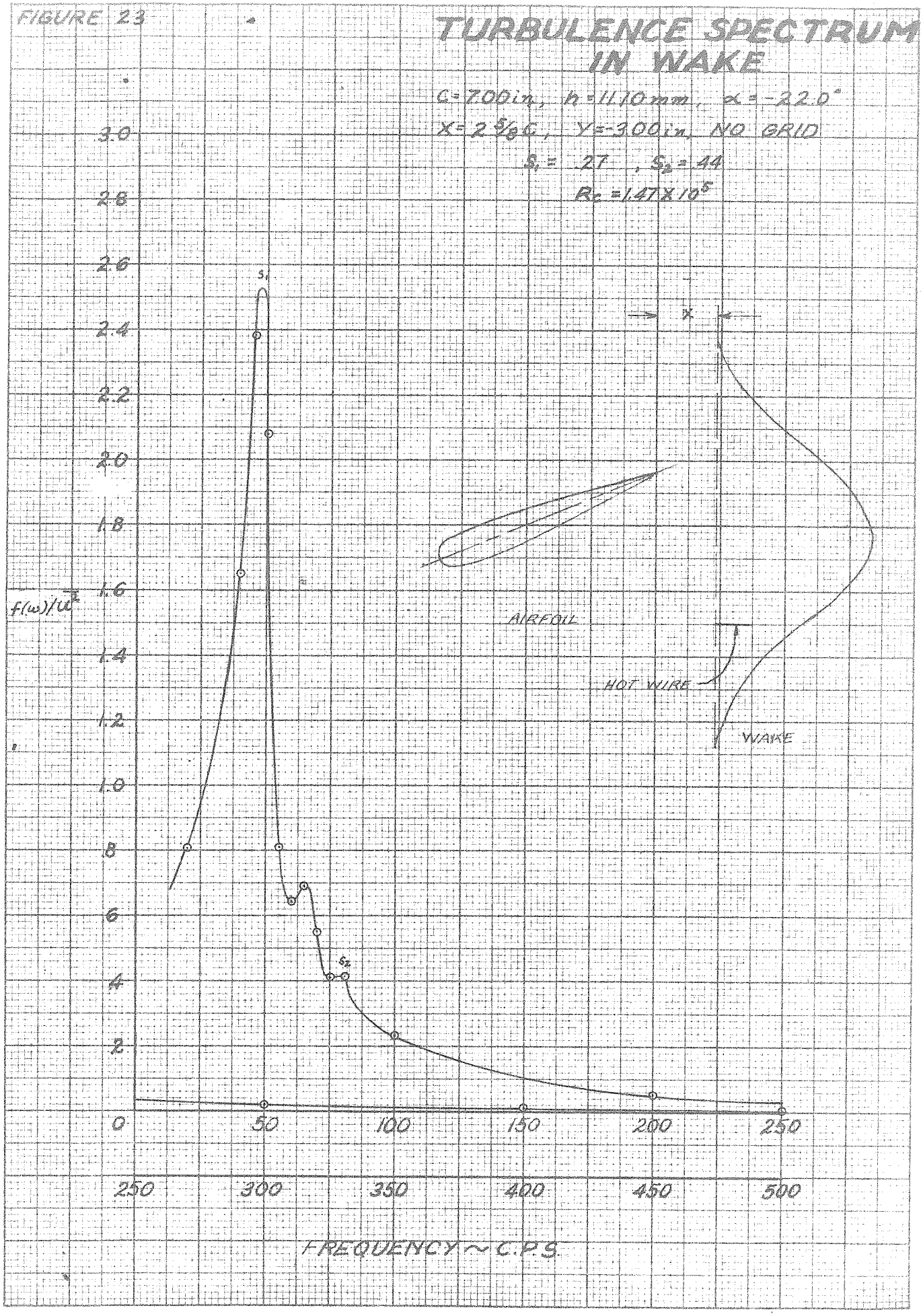

FIGURE 24

TURBULENCE SPECTRUM IN WAKE

C = 7.00 in. h = 11.10 mm, α = -22.0°

X = 2 5/8 C, Y = -6.00 in, NO GRID

S_1 = .28, S_2 = —

R_c = 1.47 X 10^5